PHYSICAL REVIEW B **74**, 094418 (2006)

Magnetic interactions in transition-metal-doped ZnO: An *ab initio* study

Priya Gopal and Nicola A. Spaldin
Materials Department, University of California, Santa Barbara, California 93106-5050, USA

(Received 28 May 2006; revised manuscript received 23 June 2006; published 15 September 2006)

We calculate the nature of magnetic interactions in transition-metal doped ZnO using the local spin density approximation and (LSDA) the LSDA+U (Coulomb interaction) method of density functional theory. We investigate the following four cases: (i) single-transition-metal-ion types (Cr, Mn, Fe, Co, Ni and Cu) substituted at Zn sites, (ii) substitutional magnetic transition-metal ions combined with additional Cu and Li dopants, (iii) substitutional magnetic transition-metal ions combined with oxygen vacancies, and (iv) pairs of magnetic ion types (Co and Fe, Co and Mn). Extensive convergence tests indicate that the calculated magnetic ground state is unusually sensitive to the k-point mesh and energy cutoff, the details of the geometry optimizations, and the choice of the exchange-correlation functional. We find that ferromagnetic coupling is sometimes favorable for single-type substitutional transition-metal ions within the LSDA. However, the nature of magnetic interactions changes when correlations on the transition-metal ion are treated within the more realistic LSDA+U method, often disfavoring the ferromagnetic state. The magnetic configuration is sensitive to the detailed arrangement of the ions and the amount of lattice relaxation, except in the case of oxygen vacancies when an antiferromagnetic state is always favored.

DOI: 10.1103/PhysRevB.74.094418 PACS number(s): 75.50.Pp

I. INTRODUCTION

Dilute magnetic semiconductors (DMSs), obtained by partial replacement of the cations in conventional semiconductors by magnetic transition-metal ions, are of current interest as potential semiconductor-compatible magnetic components for spintronic applications.[1] Early studies of DMSs focused on II-VI semiconductor hosts, such as CdSe and ZnTe;[2] since many transition metals adopt divalent ionic states, they therefore substitute readily for divalent cations such as Zn^{2+} or Cd^{2+}. However, most II-VI DMSs are antiferromagnetic or have very low ferromagnetic Curie temperatures,[3] rendering them unattractive for applications. More recently, robust ferromagnetism was observed in DMSs based on III-V semiconductors such as Mn-doped GaAs, in which Curie temperatures of ~150 K have been achieved.[4] Here, the ferromagnetic coupling between the localized Mn magnetic moments is believed to be mediated by itinerant carriers (holes) which are introduced when divalent Mn ions replace trivalent galliums[5,6] (so-called *carrier-mediated ferromagnetism*). Calculations for other materials, based on such a carrier-mediated mechanism with a high concentration (~5%) of holes, predicted above-room-temperature ferromagnetism for Mn-doped ZnO and GaN.[5]

In addition to the technological appeal of room-temperature ferromagnetism in ZnO-based DMSs, ZnO offers other desirable features as a semiconductor host. It has a direct wide-band gap of 3.3 eV,[7] and therefore finds widespread use in the optoelectronics industry.[8–10] Its strong piezoelectricity[11] is exploited in a variety of transducer applications[12] and has possible application in polarization field effect transistors.[13] And long spin coherence times, with potential spintronic applications, have recently been reported at room temperature in n-type ZnO.[14] Thus, if it could be achieved, ferromagnetic ZnO would be a highly multifunctional material with coexisting (and possibly coupled) magnetic, piezoelectric, optical, and semiconducting properties.

The predictions of high-temperature ferromagnetism[5] spawned a large number of experimental[15–25] and computational[26–32] studies of transition-metal (TM) doped ZnO. The reported experimental values of Curie temperature and magnetization show a large distribution, suggesting that the system is sensitive to preparation methods, measurement techniques, substrate choice, etc. For example, in the case of Mn-doped ZnO, while some experiments report above room temperature ferromagnetism,[20,33] others report a low ferromagnetic-ordering temperature[19,34,35] or spin-glass or paramagnetic behavior.[18,22,36] Likewise, in Co-doped ZnO, there are reports of giant magnetic moments ($\sim 6.1\mu_B$/Co),[21] high ferromagnetic-ordering temperatures with moments of $\sim 1-3\mu_B$,[16,37–39] and in some cases no ferromagnetic behavior at all.[22,25,36,40] Interestingly, the reported computational results show a similar spread of values; this arises not only from different physical approximations (choice of exchange-correlation functional, inclusion, or omission of structural relaxations), but also from the unusual sensitivity of the magnetic interactions to the convergence quality of the computations. (For a detailed review see Ref. 24.) As a result, in spite of the flurry of experimental and theoretical work, no definite conclusions have been reached regarding the nature and origin of the magnetic interactions in this system.

In this paper, we report our results of a systematic computational study of transition-metal-doped ZnO, with the goal of understanding the nature and origin of the magnetic interactions. Our emphasis is on extracting trends along the $3d$ transition-metal series, and so we first explore the effects of substitutional doping with a range of transition metals (Cr, Mn, Fe, Co, Ni, and Cu). Next, we calculate the effects of additional dopant or vacancy impurities, and finally we calculate the preferred magnetic configurations of *pairs* of different magnetic ion types. Our main finding is that the ferromagnetic state is generally disfavored in the most realistic calculations, and it is not strongly stabilized by common defects likely to be found in as-grown ZnO, or easily incorporated as dopants.

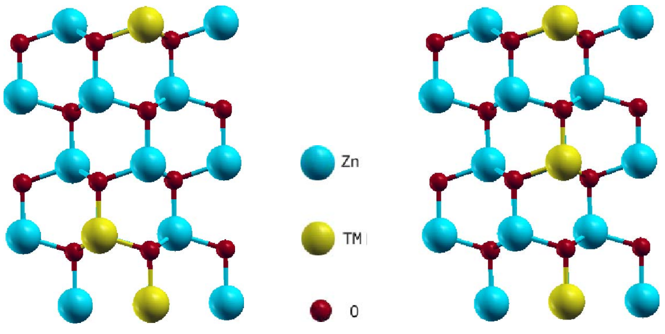

(a) near (b) far

FIG. 1. (Color online) Wurtzite supercell of ZnO with two TM ions in the (a) near and (b) far configuration. The (yellow) light-shaded spheres are the TM ions, the large (cyan) dark-shaded spheres the Zn ions, and the small (red) black spheres the O ions.

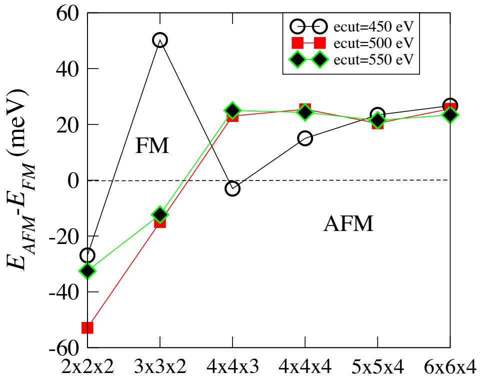

FIG. 2. (Color online) Plot of E_{AFM}-E_{FM} for $\mathrm{Zn}_{0.875}\mathrm{Co}_{0.125}\mathrm{O}$ as a function of the k-point grid and for three different plane-wave energy cutoffs (ecut).

The remainder of this paper is organized as follows. In the next section, we describe our computational and system details and outline the unusually demanding convergence behavior that we find for TM-doped ZnO. In Sec. III, we present our calculated trends across the 3d series for single-type transition-metal doping within the local spin density approximation (LSDA) and the LSDA+U method. In Sec. IV we investigate the influence of defects across the 3d series by (i) co-doping with Cu or Li and (ii) incorporation of oxygen additional oxygen vacancies. In Sec. V, we present our results for double doping (simultaneous doping of two different TM ions) in [Zn,(Co,Fe)]O and [Zn,(Mn,Co)]O. Finally, we summarize our results in Sec. VI.

II. TECHNICALITIES

A. System details

In order to achieve realistic experimental dopant concentrations (~10–30 %), we used a periodic $2\times2\times2$ wurtzite supercell of ZnO which consists of 32 atoms in a unit cell. Substitution of two Zn atoms by transition-metal ions then gives a dopant concentration of 12.5% and allows for calculation of the relative energies of ferromagnetic (FM) and antiferromagnetic (AFM) orderings. We explored two spatial arrangements, near (transition-metal atoms separated by one oxygen atom) and far (TM atoms separated by -O-Zn-O-), as shown in Fig. 1. In each case, we used the energy difference between FM and AFM ordering, $\Delta E = E_{\mathrm{AFM}}$-$E_{\mathrm{FM}}$, as an indicator of the magnetic stability (a positive ΔE implies that FM is favorable). The energy difference is defined per supercell. Equating ΔE with the thermal energy k_BT suggests room-temperature ferromagnetism should be achieved for ΔE values larger than ~30 meV.

B. Method details

Our total energy and electronic structure calculations were performed using the projector augmented wave[41] (PAW) formalism of density functional theory as implemented in the VASP package.[42–44] We used the default VASP PAW potentials with 12 valence electrons for Zn ($3d^{10}4s^2$), six for O ($2p^4 2s^2$), and $2+n$ ($3d^n 4s^2$); $n=3-9$ for the transition metals. We used a well-converged energy cutoff of 550 eV for plane-wave expansion of the PAW's, a $4\times4\times3\Gamma$-centered k-point grid, and the tetrahedron method with Blöchl[41] corrections for the Brillouin zone integrations. Note that this energy cutoff and k-point sampling are unusually high; our convergence tests (Fig. 2) indicate that qualitatively incorrect magnetic behavior often occurs for lower values. Similarly rigorous convergence parameters have been shown to be required for accurate calculations for Co-doped TiO_2.[45] For all geometry optimizations, we kept the volume of the supercell fixed to the experimental volume ($a=6.50$ Å and $c=10.41$ Å[7]) and relaxed all the internal coordinates until the Hellmann-Feynman forces were less than 10^{-3} eV/Å.

We approximated the exchange-correlation functional with both the local spin density approximation (LSDA) and the fully localized limit of the LSDA+U method.[46] Although widely used and well established for many properties, the LSDA is well known to yield incorrect behavior for strongly correlated magnetic systems, often predicting half-metallic, low spin states for systems which are actually insulating and high spin. For example, most TM monoxides are wide-band-gap antiferromagnetic insulators,[47–51] however, the LSDA finds them to be either FM metals (FeO and CoO) or small-gap semiconductors (MnO and NiO).[52] The LSDA+U method extends the LSDA by explicitly adding the on-site d-d Coulomb interaction, U, and the on-site exchange interaction, J, to the LSDA Hamiltonian, and usually gives improved results for magnetic insulators. Here we use typical values of $U=4.5$ eV and $J=0.5$ eV on all transition metals;[53–55] although a small variation in U and J across the series is expected, our choice of constant values permits a more straightforward comparison. We do not modify the LSDA ZnO electronic structure, which, therefore, shows the usual LSDA underestimation of the band gap, and shift of the Zn d state energies.

III. MAGNETIC INTERACTIONS IN DOPED ZNO

A. LSDA results

We begin by calculating the total energies of 12.5% TM-substituted ZnO within the local spin density approximation

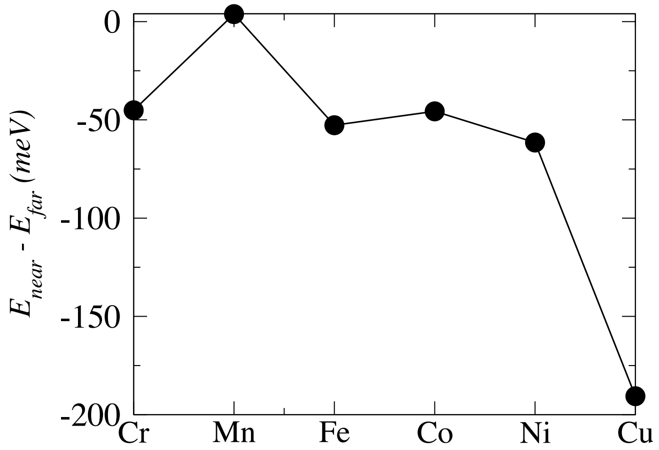

FIG. 3. LSDA energy differences ($\Delta E = E_{\text{near}}$-$E_{\text{far}}$) for substitutional TM ions. The negative energy difference indicates that the TM ions prefer to be in a near spatial configuration.

(LSDA). We reiterate that we do not expect the LSDA to give accurate magnetic behavior for this system, but present the results as a baseline for comparison with our LSDA+U results in the next section. Keeping the volume fixed at the ZnO experimental volume, we first relax all internal coordinates for near and far arrangements of the TM ions, and for both AFM and FM orderings. In Fig. 3 we show our calculated energy differences between the near and far configurations; it is clear that in all cases (except Mn, for which the energy difference is negligible) it is favorable for the TM ions to cluster together.

Figures 4(a) and 4(b) show our calculated magnetic energy differences (E_{AFM}-E_{FM}) for our range of TM dopants in the near and far spatial arrangements. First we note that our calculated magnetic orderings without ionic relaxations, which vary considerably both with the TM type and with the spatial arrangement, are consistent with earlier calculations in the literature.[17,27,56] We see, however, that the strength and sign of the magnetic interaction is highly sensitive to the ionic relaxation, which changes both the distance between the TM ions (by up to ~0.25 Å) and the TM-O-TM angle (by up to ±5%). We find no clear trends in the magnitude of relaxation, nor any direct correlation between the relaxation and the change in the magnetic interactions, across the TM series. We attribute the sensitivity in magnetic ordering to a subtle competition between antiferromagnetic superexchange (favored by 180° bond angles), ferromagnetic superexchange (favored by the 90° TM-O-TM bond angles), and AFM direct exchange (favored by short TM-TM distances).[57–59] Our results indicate that ionic relaxations must always be included in calculations to obtain meaningful results, and that even the generalization of relaxed positions from one TM ion to another should be applied with caution.[17,56] For the most realistic configurations (near, with relaxations), the LSDA suggests that doping with Cr, Fe, Co, Ni and Cu should lead to a ferromagnetic ground state.

Next (Fig. 5) we compare our calculated total densities of states (DOS) and TM 3d projected local densities of states (PDOS) for our range of TM ions in ZnO. In all cases the DOS for the FM arrangement is shown. The total DOS is represented by the gray-shaded region while the black-shaded regions represent the 3d states of the TM impurities. The majority (↑) spin states are plotted along the negative x direction, and the minority (↓) states are plotted along the positive x direction. The energies are reported relative to the Fermi energy ($E_f = 0$). For comparison, the DOS of undoped ZnO is also shown, with the Fermi energy set to the top of the valence band.

Comparison with the ZnO DOS identifies the broad (~4–5 eV) band just below the Fermi energy as derived largely from the O 2p states, with the narrow Zn 3d band just below and slightly overlapping with the O bands. The bottom of the conduction band is composed largely of Zn 4s states, and the band gap (~0.78 eV) shows the usual LSDA underestimation.

In all cases, the exchange-split TM 3d states form fairly narrow bands in the region of the gap. The exchange splitting (~2 eV) is consistently larger than the crystal-field splitting (~0.5 eV) which splits each spin manifold into lower energy doubly degenerate e and higher energy triply degenerate t states. We observe the following trends, which are consistent with the crystal chemistry of 3d transition-metal oxides:

(i) The energy of the TM 3d states relative to the top of the valence band shifts down in energy on moving right

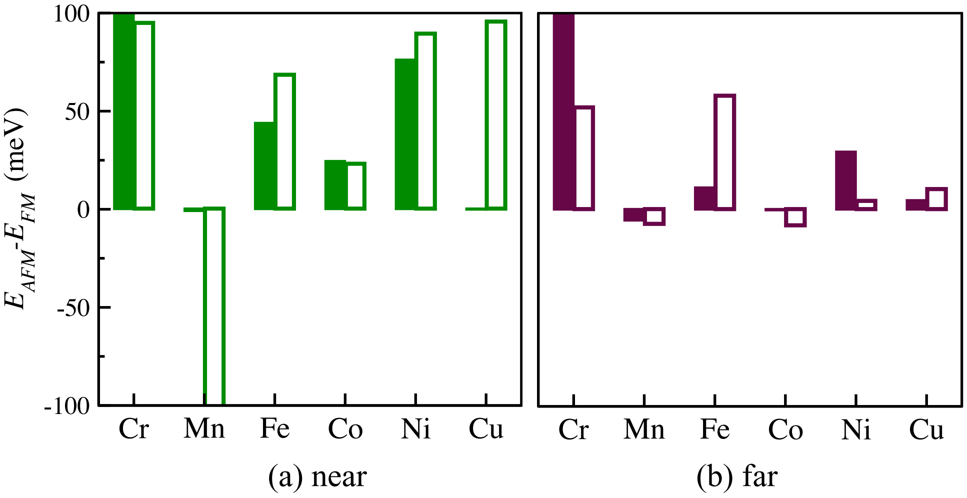

(a) near (b) far

FIG. 4. (Color online) LSDA energy differences ($\Delta E = E_{\text{AFM}}$-$E_{\text{FM}}$) for substitutional TM ions in ZnO for (a) near and (b) far spatial configurations. In both (a) and (b), the filled bars represent the case when the ionic coordinates are not relaxed and the unfilled bars represent the case when the ionic coordinates are relaxed. Lines at $\Delta E = 0$ indicate that FM and AFM orderings are equivalent in energy.

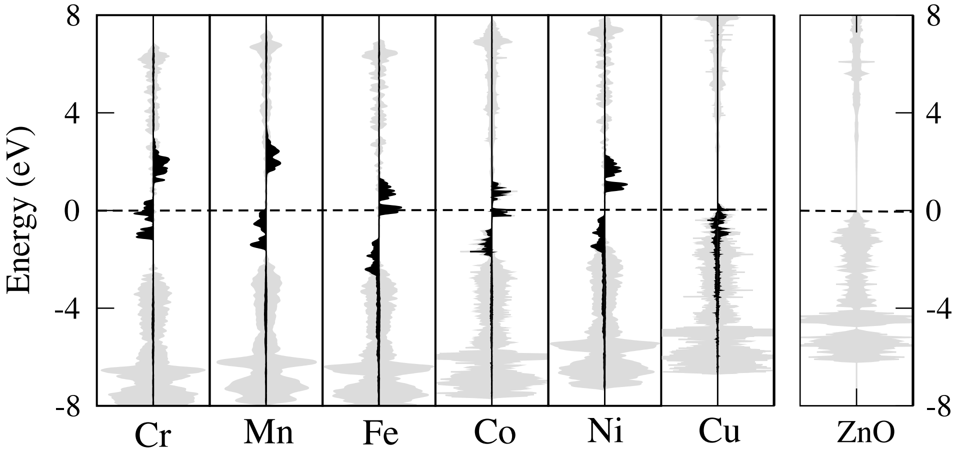

FIG. 5. DOS and PDOS of TM-doped ZnO with the TM atoms in the near spatial configuration calculated within the LSDA. The black-shaded regions show the TM *d* states, and the gray-shaded regions show the total DOS. For clarity, the TM *d* states are scaled by a factor of two. Also shown (right panel) is the DOS for undoped ZnO.

across the 3*d* series (from Cr to Cu). As a consequence, the Cr states are somewhat hybridized with the bottom of the conduction band (this is likely a result of the LSDA underestimation of the ZnO band gap), the Fe and Co states are largely midgap, and the Cu states are hybridized with the top of the valence band.

(ii) The calculated DOSs (Fig. 5) are consistent with the Hund's rule predictions for isolated TM ions, with only majority-spin (↑) states occupied for Cr and Mn, and occupation of the minority-spin (↓) states increasing Fe to Co to Ni to Cu. Also, the exchange splitting decreases on moving to the right across the 3*d* series.

(iii) The $(d^5)^{\uparrow}$ Mn^{2+} and $(d^5)^{\uparrow}$ $(d^2)^{\downarrow}$ Co^{2+} ions lead to insulating behavior; the other ions have partially filled *d* manifolds and a finite density of states at the Fermi level.

(iv) The variation in magnetic moments across the 3*d* series reflects the decrease in exchange splitting, and the increase in the number of electrons, with the local magnetic moments (obtained by integrating up to a Wigner-Seitz radius of 1.4 Å)[60] on the TM ion as follows (in units of μ_B): 3.04 (Cr), 4.31 (Mn), 3.51 (Fe), 2.44 (Co), 1.49 (Ni) and 0.55 (Cu).

These LSDA results are consistent with earlier LSDA calculations,[17,27,29] and also with some experimental reports.[20] Since the LSDA is known to underestimate the band gaps and exchange splittings in magnetic systems, we withhold a detailed analysis of the band structures until the following section, where we repeat our calculations with the inclusion of correlations at the level of the LSDA+U method.

B. LSDA+*U*

Next we repeat the suite of calculations described above, with the correlation on the 3*d* TM ions treated within the LSDA+U scheme.[46] Here we present results obtained using typical values of $U=4.5$ eV and $J=0.5$ eV; in the Appendix we discuss the U dependence of our calculated properties.

First, in Fig. 6 we present our calculated LSDA+U DOSs of TM-doped ZnO. Although all the trends across the series remain the same as in the LSDA, the addition of the Hubbard U term, as expected, causes an increased splitting between the filled and empty orbitals in the TM *d* manifold. The exchange splitting is now increased to ~4 eV, and the crystal-field splitting increases to ~1 eV. The TM *d* states, which were localized in the gap in the LSDA, now shift down in energy and hybridize strongly with the O 2*p* states. Note that our results agree with earlier LSDA+U calculations on Mn and Co-doped ZnO by Chanier *et al.*[61] Comparing the DOS of Fe and Ni, we observe a transition from half-metallic to insulating when going from the LSDA to LSDA+U. This is directly reflected in the magnetic intera-

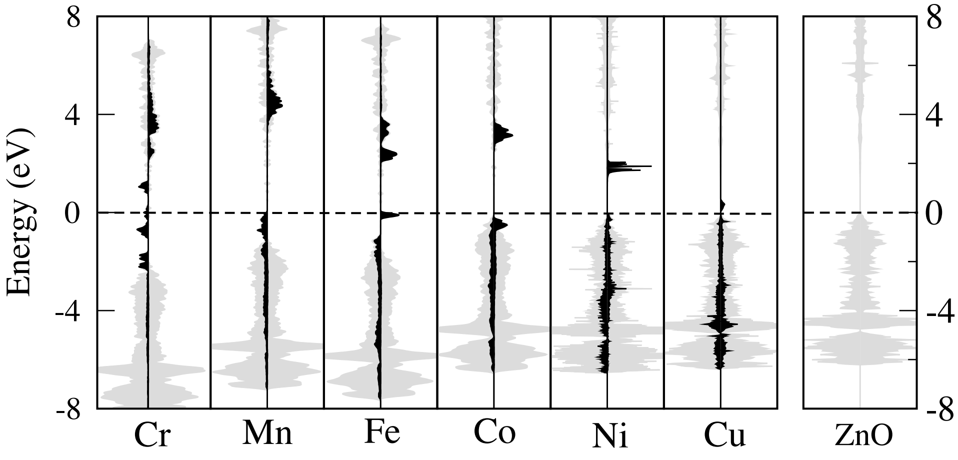

FIG. 6. DOS and PDOS of TM-doped ZnO with TM atoms in the near spatial configuration calculated within the LSDA+U method. The black-shaded regions show the TM *d* states, and the gray-shaded regions show the total DOS. For clarity, the TM *d* states are scaled by a factor of two. Also shown (right panel) is the DOS for undoped ZnO.

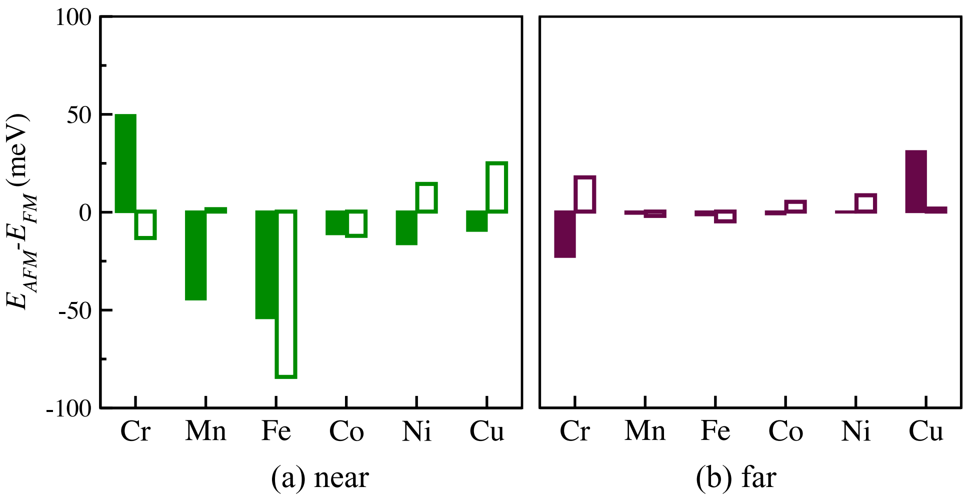

(a) near (b) far

FIG. 7. (Color online) LSDA $+U$ energy difference, $\Delta E = E_{\mathrm{AFM}}$-$E_{\mathrm{FM}}$, for substitutional TM ions in ZnO represented for (a) near and (b) far spatial configurations. The filled bars show the energies when the ions are not relaxed and the unfilled bars give the values for when relaxations are included. Lines at $\Delta E=0$ indicate that FM and AFM orderings are equivalent in energy.

tion strength. For example, in Fe and Ni, the long-range interaction vanishes and the interaction strength decreases. We also calculated the magnetic moments on the TM ion as follows (in units of μ_B): 3.40 (Cr), 4.41 (Mn), 3.54 (Fe), 2.56 (Co), 1.63 (Ni), and 0.65 (Cu). The magnetic moments are slightly larger compared to the LSDA values. Next we compare the total energies of the FM and AFM magnetic orderings in the near and far spatial configurations. In all cases, all the ionic coordinates are relaxed within the LSDA+U scheme. Figures 7(a) and 7(b) show the energy difference between the FM and AFM states, (E_{AFM}-E_{FM}), for near and far arrangements for the various TM ions. As in the LSDA case, ΔE shows a strong dependence on the spatial arrangement of the dopant ions, as well as on the extent of ionic relaxations included in the calculation. In all cases, the sign and magnitude of the interactions are strikingly different from those obtained within the LSDA, with a general trend to reduced ferromagnetism. For the energetically favorable near case, only Ni and Cu dopants show a tendency to ferromagnetic ordering when ionic relaxations are included in the calculation.

IV. INFLUENCE OF DEFECTS

A. Possible *p*-type dopants; Cu and Li with TM in ZnO

Given that our calculations containing single types of substitutional dopants are unable to reproduce the experimentally reported ferromagnetism, we next search for other impurities that could mediate the ferromagnetic ordering. Since the original predictions of high Curie temperature in Mn-doped ZnO[5] assumed high hole concentrations, we first include additional dopants which might introduce *p*-type carriers. Some experimental[62] and theoretical studies[56] have suggested that Cu could provide holes when doped into ZnO. Although our observation of a magnetic moment on Cu makes acceptor behavior unlikely, earlier LSDA calculations on Cu-doped ZnO found a band structure consistent with this model, and an enhanced tendency to ferromagnetism.[29] Lithium has also been suggested as a possible *p*-type dopant in ZnO.[63] Li has an electronic configuration of $1s^2$, $2s^1$, and tends to form a singly charged cation ($1s^2\ 2s^0$) with an ionic radius (0.59 Å) close to that of Zn^{2+}.

In this section, we calculate the effects of co-doping TM-doped ZnO with Cu or Li, again within the LSDA+U method, using the same convergence and U and J parameters as described above. Our calculated ΔE values are shown in Fig. 8. In all cases the concentration of the Cu or Li was 6.25% (one additional dopant in 16 cations), and the additional dopant was placed far away from the TM ion in ZnO. In the case of Cu as a defect atom, we have the AFM and FM arrangements describe the relative orderings of the two like TM (Cr, Mn, Fe, Co, Ni) atoms.

It is clear that, in contrast with earlier LSDA calculations, co-doping with Cu does not strongly enhance the tendency towards ferromagnetism within the LSDA+U method, which yields an antiferromagnetic ground state in most cases, and a weakly ferromagnetic state for Cr and Ni. Co-doping with Li, however, is more favorable for ferromagnetism, and in some cases should lead to above-room-temperature ferromagnetism. This is particularly intriguing in light of recent reports of ferroelectricity in Li-doped ZnO,[64,65] suggesting the possibility of engineering a multiferroic material with simultaneous ferromagnetism and ferroelectricity. However, none of our calculated Li-doped materials is insulating, which is a requirement for ferroelectricity.

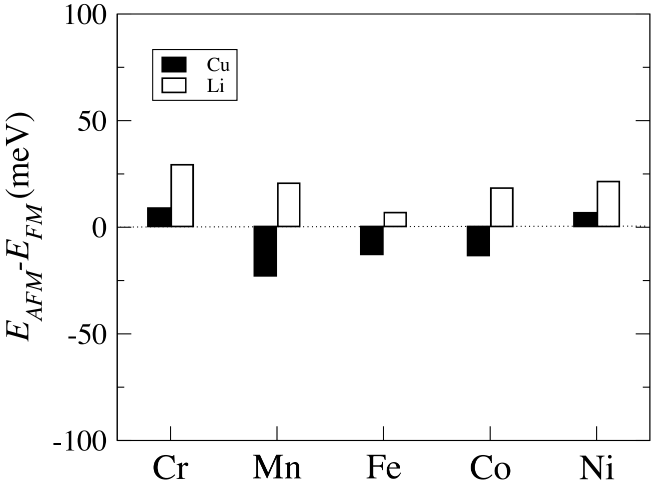

FIG. 8. E_{AFM}-E_{FM} for TM-doped ZnO with 6.25% Cu/Li.

B. O vacancies: Zn(TM,V_o)O

Next, we combine substitutional TM ions with oxygen vacancies, which are believed to be the most common native defects in ZnO.[63,66,67] There is some experimental evidence associating the presence of oxygen vacancies with the existence of ferromagnetism in TM-doped ZnO. For example, Venkatesan *et al.*[16] reported a correlation between the magnitude of Co magnetic moments and the oxygen partial pressure during annealing, with higher oxygen partial pressure reducing the amount of magnetization. In addition, Kittilsved *et al.*[23] report room-temperature ferromagnetism in Co-doped ZnO nanocrystals with oxygen-containing surfaces, and propose that oxygen vacancies mediate the magnetic interactions. Other experiments observe a change in the magnetization in samples on annealing in a reducing atmosphere which they attribute to oxygen vacancies.[68] As a result of this reported correspondence between the presence of oxygen vacancies and the existence of ferromagnetism, a model has been proposed in which ferromagnetism is mediated by carriers in a spin-split impurity band derived from extended donor orbitals.[16,37] The validity of the model rests on the formation of an oxygen-vacancy-derived donor impurity band close to the ZnO conduction band edge, which hybridizes with the spin-polarized TM 3*d* band. If the Fermi energy lies within this hybrid oxygen vacancy/TM 3*d* spin-polarized band, a carrier-mediated ferromagnetism should be favorable. Here we calculate the relative energies of the oxygen impurity levels and the transition metal 3*d* states across the TM series, in order to investigate the applicability of this model. Indeed, by simple charge neutrality arguments, removal of a neutral oxygen atom should leave two unbonded electrons associated with the vacancy, provided that the Zn remains in a Zn^{2+} state. We note, however, that recent first-principles calculations[69] found oxygen vacancies to be deep donors in ZnO, and therefore, unavailable for carrier mediation.

We introduce a single O vacancy as far as possible from the TM ions which are again in both the near and far configurations. The energy difference (E_{AFM}-E_{FM}) is plotted in Fig. 9. We see that the AFM state is stable in all cases, consistent with previous computations for Co-doped ZnO with a neutral oxygen vacancy.[17,29,30]

In Fig. 10 we show our calculated DOSs for the entire series. We see a shift of the Fermi energies relative to those in the absence of oxygen vacancies, but no other striking changes in band structure. In particular, it is clear that the Fermi level does not lie in a hybridized TM 3*d*-O 2*p* impurity band for any case. Therefore, our band structures are not consistent with those required to mediate ferromagnetism within the model proposed above for our choice of concentration of oxygen vacancy; they are, however, consistent with our calculated AFM ground states. We note, however, that a different oxygen vacancy concentration could shift the Fermi level and make the band structure consistent with the vacancy-induced spin-split impurity band model.[37]

The calculated magnetic moments (in units of μ_B) for each TM ion in the presence of the oxygen vacancy are 3.54 (Cr), 4.36 (Mn), 3.66 (Fe), 2.64 (Co) and 1.68 (Ni), largely unchanged from the LSDA+U values without the oxygen vacancy. This indicates that the two electrons from the oxygen vacancy are localized at the vacancy and do not influence the occupancy of the TM *d* states. Finally, we point out that we have considered only neutral oxygen vacancies here. A recent first-principles study suggests that positively charged oxygen vacancies might be more successful for mediating ferromagnetism in Co-doped ZnO.[30]

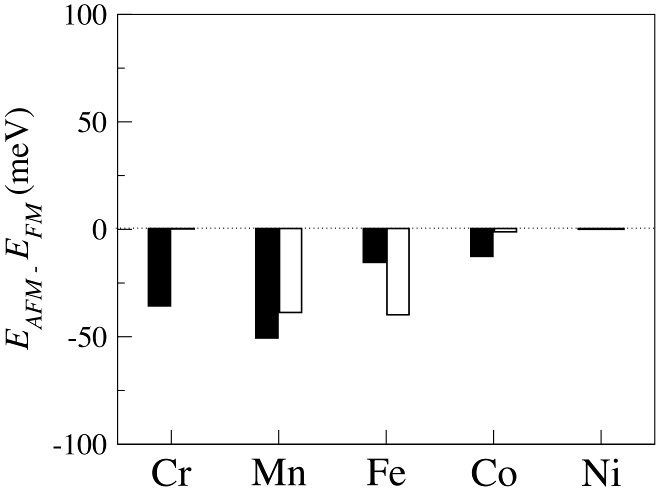

FIG. 9. E_{AFM}-E_{FM} for the range of TM ions in the presence of an oxygen vacancy. The filled and unfilled bars represent the cases when the TM ions are near and far from each other, respectively. In both cases the oxygen vacancy is placed as far as possible from the TM ions.

C. Other defects

Next, we study the effect of a range of experimentally plausible defects—Zn vacancies (V_{Zn}), octahedral Zn interstitials (Zn_i), TM interstitials (Co_i), and Li interstitials (Li_i)—on the magnetic interactions. Rather than scanning the entire range of transition-metal dopants, we use Co-doped ZnO as our test system, since it is the most widely studied both experimentally[15,16,24,70,71] and theoretically.[17,29,30,56,72] Figure 11 shows our calculated $\Delta E = E_{\mathrm{AFM}}$-$E_{\mathrm{FM}}$ for the near spatial arrangement, with the vacancies placed as far as pos-

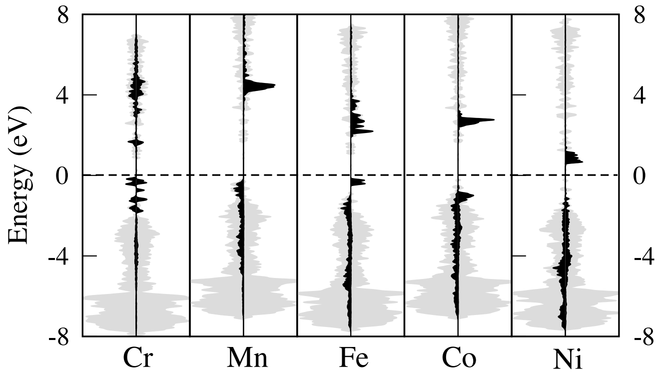

FIG. 10. DOS and PDOS for TM-doped ZnO (near spatial arrangement and the FM state) in the presence of oxygen vacancies.

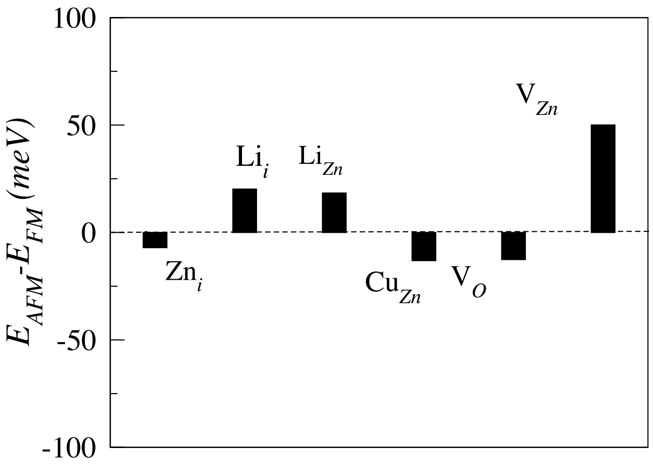

FIG. 11. E_{AFM}-E_{FM} for ZnO doped with Co and a range of other defects.

sible from the Co ions. Our previously reported values for substitutional Li (Li_{Zn}), substitutional Cu (Cu_{Zn}), and oxygen vacancies (V_O) are also shown for completeness.

Perhaps the most important result is that, as in the case of substituional Li reported above, interstitial Li also stabilizes the ferromagnetic state. This is significant since Li impurities are likely to be incorporated both in substitutional and interstitial sites during growth, and avoiding competing antiferromagnetic interactions is desirable. We also see that Zn vacancies are favorable for ferromagnetism, consistent with previous reports in the literature.[17,29,30] The other defects studied do not stabilize the ferromagnetic state.

V. SIMULTANEOUS DOPING OF CO WITH OTHER TM IONS

Finally, we calculate the properties of ZnO doped with both Co and an additional TM ion (Mn or Fe). There has been some experimental work on such co-doped ZnO-based DMSs. Cho *et al.*[71] reported room-temperature magnetism with a saturation magnetization of 5.4 emu/g (corresponding to $\sim 1\mu_B$ for CoFe pair) for $Zn_{1-x}(Fe_{0.5},Co_{0.5})_xO$ ($x=0.15$) films fabricated by reactive magnetron co-sputtering. Han *et al.*[62] also reported room temperature magnetism for $Zn_{1-x}(Fe_{1-y},Cu_y)_xO$ bulk samples with $T_C \sim 550$ K. On the theory side, Park and Min[26] calculated the electronic structures and magnetic properties of (Fe,Co) and (Fe,Cu) doped ZnO at 12.5% doping. They reported a tendency to form FM Fe-O-Cu clusters, and argued that ferromagnetism should arise from a double exchange, whereas the absence of clustering found for (Fe,Co)-doped ZnO would require a different mechanism for ferromagnetism.

Here we explore the possibility of ferr*i*magnetic (FiM) ordering, in which the magnetic moments of one TM-ion type are antiparallel to those of the other TM-ion type, but a net magnetization arises from incomplete cancellation of the magnetic moments. For each system [Zn(Co,Fe)O and Zn(Co,Mn)O] we calculate the total energies of the FM, AFM, and FiM magnetic orderings as shown in Fig. 12 with TM ions of different type in the near arrangement. We use a $4\times4\times2$ wurtzite supercell with 64 atoms (double the size of the previous studies), which allows the permutations shown in Fig. 12 at a TM-ion concentration of 12.5%. Within this constrained spatial arrangement, we find that in both systems the FiM ordering is the most stable arrangement by 200 meV for [Zn,(Co,Fe)]O, and by 57 meV for [Zn,(Co,Mn)]O; the corresponding magnetic moments per supercell are $1.11\mu_B$ for [Zn,(Co,Fe)]O and $1.98\mu_B$ for [Zn,(Co,Fe)]O which agrees well with the experimentally reported values.[71] While ferrimagnetism overcomes the problem of cancellation of magnetic moments by superexchange-driven antiparallel alignment, it, of course, requires that ions of different types cluster together while those of the same type remain distant; this might be difficult to achieve experimentally.

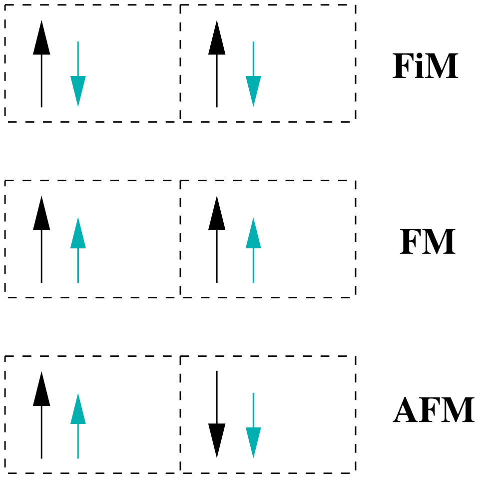

FIG. 12. (Color online) A schematic of the different magnetic orderings investigated in this work. The black arrows represent the magnetic moments of the Co ions while the blue (gray) arrows represent the magnetic moments of the other TM ions (Mn or Fe).

For completeness, we show the DOSs of FiM $Zn_{0.875}(Co_{0.5},M_{0.5})_{0.125}O$ ($M=$Mn,Fe) in Fig. 13. The [Zn,(Co,Mn)] DOS is almost an exact superposition of the separate (Zn,Mn)O and (Zn,Co)O DOSs. Interestingly and unlike either (Zn,Fe)O or (Zn,Co)O, the [Zn,(Fe,Co)]O system is metallic because of a narrow spin-polarized impurity band at the Fermi level.

VI. SUMMARY

In summary, we have performed a systematic study of the magnetic behavior of TM-doped ZnO for a range of TM ions and defects. Our main result is the absence, in general, of a tendency for pairs of TM ions substituted for Zn to order ferromagnetically; in most cases AFM ordering is more favorable. Ferromagnetic ordering of TM ions is not induced by the addition of substitutional Cu impurities nor by oxygen vacancies. Incorporation of interstitial or substitutional Li is favorable for ferromagnetism, as are Zn vacancies. On a technical note, we find that the calculated magnetic behavior is strongly dependent both on the computational details (with ferromagnetism disfavored by improved convergence) and

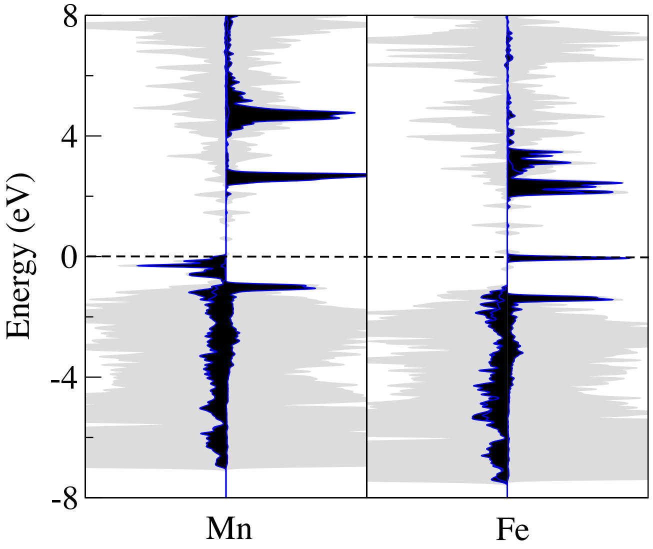

FIG. 13. (Color online) DOSs and PDOSs of 3*d* states for ferrimagnetic $Zn_{0.875}(Co_{0.5}Mn_{0.5})_{0.125}O$ and $Zn_{0.875}(Co_{0.5}Fe_{0.5})_{0.125}O$. The blue-shaded region represents the *d* states of the Co ions while the black-shaded region represents the *d* states of the TM ions.

on the choice of exchange-correlation functional (with ferromagnetism disfavored by the more appropriate LSDA+U method). This observation explains the large spread of computational results in the literature.

ACKNOWLEDGMENTS

This work was funded by the Department of Energy, Grant No. DE-FG03-02ER4598, and was partially supported by the MRSEC Program of the National Science Foundation under Award No. DMR05-20415. The authors thank Rebecca Janisch for useful discussions.

APPENDIX: DEPENDENCE OF PROPERTIES ON CHOICE OF U: THE EXAMPLE OF CO-DOPED ZNO

Here we illustrate the sensitivity of our results to the magnitude of the U parameter with calculations of the energy difference, E_{AFM}-E_{FM} and total and orbital-resolved densities of states, as a function of U in the (Zn,Co)O system. The U dependence of the properties are plotted in Fig. 14. Figure 14 (upper panel) shows E_{AFM}-E_{FM} for the LSDA case [with $U=0$. (i)], for U on the Co *d* states ranging from 4 to 6 eV [points (ii), (iii), and (iv)] and with a U of 4 eV on Co and 4.5 eV on Zn *d* states, respectively (v). Two conclusions can be drawn from the plot. First, the sign of the magnetic interaction changes from LSDA to LSDA+U in the near case making the AFM ordering more stable. The AFM then remains stable for all U values tested. Second, the U on the Co ion dominates the magnetic interaction; the energy differences in cases (ii) and (v) are very close, indicating that correlations on the Zn *d* states do not significantly affect the magnetic interactions. Figure 14 (lower panel) shows the DOS and Co *d* PDOS in Co-doped ZnO for the same range of U values. We see that, as expected, the exchange splitting between occupied majority states, and unoccupied minority states increases with U; as a consequence, the majority occupied states move down into the valence band and hybridize more strongly with the O 2*p* states as U is increased. Adding a U of 4.5 eV on the Zn also lowers the energy of the Zn *d* states.

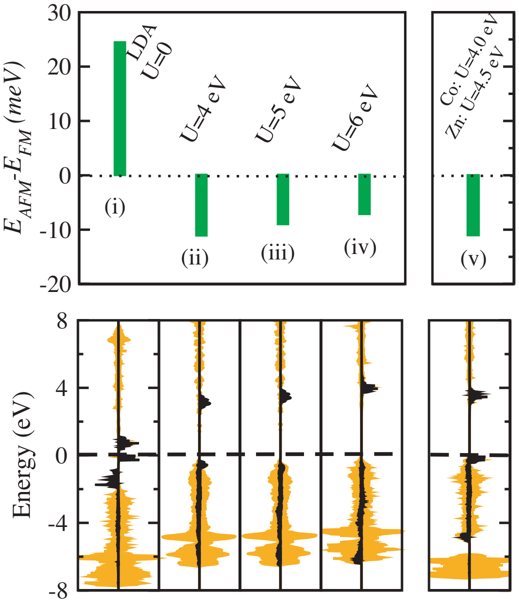

FIG. 14. (Color online) (Upper panel) Total energy difference (E_{AFM}-E_{FM}) for 12.5% Co with Co atoms in the near case in ZnO for various U values on the Co *d* states. The last bar gives this energy difference with U=4 eV on Co 3*d* and 4.5 eV on Zn 3*d* states. (Lower panel) Total DOS of (Zn,Co)O and PDOS of Co *d* states for a range of U values. The light-shaded regions represent the total DOS while the black-shaded regions correspond to the 3d states of Co ion.

---

[1] H. Ohno, Science **281**, 951 (1998).
[2] J. Furdyna, J. Appl. Phys. **64**, R29 (1988).
[3] H. Saito, W. Zaets, S. Yamagata, Y. Suzuki, and K. Ando, J. Appl. Phys. **91**, 8085 (2002).
[4] K. Ku, J. Potashnik, R. Wang, S. Chun, P. Schiffer, N. Samarth, M. Seong, A. Mascarenhas, E. Johnston-Halperin, and R. Myers, Appl. Phys. Lett. **82**, 2302 (2003).
[5] T. Dietl, H. Ohno, F. Matsukara, J. Cibert, and D. Ferrand, Science **287**, 1019 (2000).
[6] S. Sanvito, P. Ordejon, and N. A. Hill, Phys. Rev. B **63**, 165206 (2001).
[7] *Condensed Matter*, Landolt-Börnstein, New Series, Group III (Springer-Verlag, Heidelberg, 2002).
[8] D. Norton, Y. Heo, M. Ivill, K. Ip, S. Pearton, M. Chisholm, and

T. Steiner, Mater. Today **6**, 34 (2004).
[9] D. C. Look, Mater. Sci. Eng., B **80**, 383 (2001).
[10] D. C. Look, R. Jones, J. Sizelove, N. Garces, N. Giles, and L. Haliburton, Phys. Solid State **195**, 171 (2003).
[11] N. A. Hill and U. V. Waghmare, Phys. Rev. B **62**, 8802 (2000).
[12] V. E. Wood and A. E. Austin, *Magnetoelectric Interaction Phenomena in Crystals* (Gordon and Breach, New York, 1975).
[13] P. Gopal and N. A. Spaldin, J. Electron. Mater. **35**, 538 (2006).
[14] S. Ghosh, V. Sih, W. H. Lau, D. D. Awschalom, S. Y. Bae, S. Wang, S. Vaidya, and G. Chapline, Appl. Phys. Lett. **86**, 232507 (2005).
[15] K. Ueda, H. Tabata, and T. Kawai, Appl. Phys. Lett. **79**, 988 (2001).
[16] M. Venkatesan, C. B. Fitzgerald, J. G. Lunney, and J. M. D. Coey, Phys. Rev. Lett. **93**, 177206 (2004).
[17] M. H. F. Sluiter, Y. Kawazoe, P. Sharma, A. Inoue, A. R. Raju, C. Rout, and U. V. Waghmare, Phys. Rev. Lett. **94**, 187204 (2005).
[18] T. Fukumura, Z. Jin, A. Ohtomo, H. Koinuma, and M. Kawasaki, Appl. Phys. Lett. **75**, 3366 (1999).
[19] S. Jung, S. J. An, G. C. Yi, C. Jung, S.-I. Lee, and S. Cho, Appl. Phys. Lett. **80**, 4561 (2002).
[20] P. Sharma, A. Gupta, K. V. Rao, F. J. Owens, R. Sharma, R. Ahuja, J. M. Osorio-Guillen, and G. A. Gehring, Nat. Mater. **2**, 673 (2003).
[21] C. Song, K. W. Geng, F. Zeng, X. B. Wang, Y. X. Shen, F. Pan, Y. N. Xie, T. Liu, H. T. Zhou, and Z. Fan, Phys. Rev. B **73**, 024405 (2006).
[22] A. S. Risbud, N. A. Spaldin, Z. Q. Chen, S. Stemmer, and R. Seshadri, Phys. Rev. B **68**, 205202 (2003).
[23] K. R. Kittilsved, N. S. Norberg, and D. R. Gamelin, Phys. Rev. Lett. **94**, 147209 (2005).
[24] R. Janisch, P. Gopal, and N. A. Spaldin, J. Phys.: Condens. Matter **17**, R657 (2005).
[25] S. Thota, T. Dutta, and J. Kumar, J. Phys.: Condens. Matter **18**, 2473 (2006).
[26] M. S. Park and B. I. Min, Phys. Rev. B **68**, 224436 (2003).
[27] K. Sato and H. Katayama-Yoshida, J. Appl. Phys. **39**, L555 (2000).
[28] L. M. Sandratskii and P. Bruno, Phys. Rev. B **73**, 045203 (2006).
[29] N. A. Spaldin, Phys. Rev. B **69**, 125201 (2004).
[30] C. H. Patterson, cond-mat/0512101 (unpublished).
[31] L. Petit, T. C. Schulthess, A. Svane, Z. Szotek, W. M. Temmerman, and A. Janotti, Phys. Rev. B **73**, 045107 (2006).
[32] E.-C. Lee and K. Chang, Phys. Rev. B **69**, 085205 (2004).
[33] Y. W. Heo, M. P. Ivill, K. Ip, D. P. Norton, and S. Pearton, Appl. Phys. Lett. **84**, 2292 (2003).
[34] Y. W. Yoon, S. B. Cho, S. C. We, B. J. Yoon, S. Suh, S. H. Song, and Y. J. Shin, J. Appl. Phys. **93**, 7879 (2003).
[35] J. Kim, W. K. Choo, H. Kim, D. Kim, and Y. Ihm, J. Korean Phys. Soc. **42**, S258 (2003).
[36] S. Kolesnik, B. Dabrowski, and J. Mais, J. Appl. Phys. **95**, 2582 (2004).
[37] J. M. D. Coey, M. Venkatesan, and C. Fitzgerald, Nat. Mater. **4**, 173 (2005).
[38] U. Özgür, Y. I. Alivov, C. Liu, A. Teke, M. A. Reshchikov, S. Dogan, V. Avrutin, S. J. Cho, and H. Morkoc, J. Appl. Phys. **98**, 041301 (2005).
[39] J. Shim, T. Hwang, J. Park, S. J. Han, and Y. Jeong, Appl. Phys. Lett. **86**, 082503 (2005).
[40] K. Ando, H. Saito, Z. Jin, F. Fukumura, M. Kawasaki, Y. Matsumato, and H. Koinuma, J. Appl. Phys. **89**, 7284 (2001).
[41] P. E. Blöchl, Phys. Rev. B **50**, 17953 (1994).
[42] G. Kresse and J. Furthmüller, Phys. Rev. B **54**, 11169 (1996).
[43] G. Kresse and J. Furthmüller, Comput. Mater. Sci. **6**, 15 (1996).
[44] G. Kresse and D. Joubert, Phys. Rev. B **59**, 1758 (1999).
[45] R. Janisch and N. A. Spaldin, Phys. Rev. B **73**, 035201 (2006).
[46] V. Anisimov, F. Aryasetiawan, and A. Lichtenstein, J. Phys.: Condens. Matter **9**, 767 (1997).
[47] R. Powell and W. E. Spicer, Phys. Rev. B **2**, 2182 (1970).
[48] W. C. Messick, L. Walker, and R. Glosser, Phys. Rev. B **6**, 3941 (1972).
[49] G. Sawatsky and J. Allen, Phys. Rev. Lett. **53**, 2239 (1984).
[50] S. Hüfner, I. Sander, F. Reinert, and H. Schnitt, J. Phys. B **86**, 207 (1992).
[51] J. v. Elp, H. Eskes, P. Kuiper, and G. A. Sawatsky, Phys. Rev. B **45**, 1612 (1992).
[52] K. Terakura, T. Oguchi, A. R. Williams, and J. Kübler, Phys. Rev. B **30**, 4734 (1984).
[53] V. I. Anisimov, J. Zaanen, and O. K. Andersen, Phys. Rev. B **44**, 943 (1991).
[54] W. E. Pickett, S. C. Erwin, and E. C. Ethridge, Phys. Rev. B **58**, 1201 (1998).
[55] M. Cococcocioni and S. de Gironcoli, Phys. Rev. B **71**, 035105 (2005).
[56] M. S. Park and B. I. Min, Phys. Rev. B **68**, 224436 (2003).
[57] P. W. Anderson, Phys. Rev. **79**, 350 (1950).
[58] J. B. Goodenough, Phys. Rev. **100**, 564 (1955).
[59] J. Kanamori, J. Phys. Chem. Solids **10**, 87 (1958).
[60] R. D. Shannon and C. T. Prewitt, Acta Crystallogr., Sect. A: Cryst. Phys., Diffr., Theor. Gen. Crystallogr. **32**, 751 (1976).
[61] T. Chanier, M. Sargolzaei, I. Opahle, R. Hayn, and K. Koepernik, Phys. Rev. B **73**, 134418 (2006).
[62] S. J. Han, J. W. Song, C. H. Yang, C. H. Park, J. H. Park, Y. H. Jeong, and K. W. Rhite, Appl. Phys. Lett. **81**, 4212 (2002).
[63] A. F. Kohan, G. Ceder, D. Morgan, and C. G. van de Walle, Phys. Rev. B **61**, 15019 (2000).
[64] A. Onodera, K. Yoshio, H. Satoh, H. Yamashita, and N. Sakagami, J. Appl. Phys. **1998**, 5315 (1998).
[65] T. Nagata, T. Shimura, Y. Nakano, A. Ashida, N. Fujimura, and T. Ito, J. Appl. Phys. **40**, 5615 (2001).
[66] S. B. Zhang, S. H. Wei, and A. Zunger, Phys. Rev. B **63**, 075205 (2001).
[67] F. Tuomisto, K. Saarinen, D. C. Look, and G. C. Farlow, Phys. Rev. B **72**, 085206 (2005).
[68] M. N. Kahn, S. K. Hasanain, M. Kobayashi, Y. Ishida, A. Fujimori, S. Buzby, and S. Ismat, Nanotechnology **17**, 2675 (2006).
[69] A. Janotti and C. G. Van de Walle, Appl. Phys. Lett. **87**, 122102 (2005).
[70] S. G. Yang, A. B. Pakhmov, S. T. Hung, and C. Y. Wong, IEEE Trans. Magn. **38**, 2877 (2002).
[71] Y. M. Cho, W. K. Choo, H. Kim, D. Kim, and Y. Ihm, Appl. Phys. Lett. **80**, 3358 (2002).
[72] E. Lee and K. J. Chang, Phys. Rev. B **69**, 085205 (2004).